Eur. Phys. J. D (2024) 78:17
https://doi.org/10.1140/epjd/s10053-024-00805-x

THE EUROPEAN PHYSICAL JOURNAL D

Regular Article - Atomic and Molecular Collisions

Positron scattering from krypton and xenon

J. R. Machacek[a] and R. P. McEachran[b]

Research School of Physics, Australian National University, Canberra, ACT 0200, Australia

Received 16 October 2023 / Accepted 2 January 2024 / Published online 9 February 2024

Abstract. A cross section set is reported for positron scattering from krypton and xenon over the energy range from zero to 1 keV using the relativistic optical potential method. This set includes elastic, positronium formation, excitation, direct ionization, and grand total cross sections. They are compared to the recommended results of Ratnavelu et al. (J Phys Chem Ref Data 48:023102, 2019). The positronium formation cross section reported is represented by the sum obtained by successively lowering the ionization threshold to coincide with those for formation into the four lowest energy levels of positronium.

1 Introduction

Positron scattering from atomic targets has been studied for many years both experimentally and theoretically with the noble gases being of particular interest [11]. The only open channel at low energies is that for elastic scattering. Consequently, early theoretical calculations were generally confined to this region. Above this region, the positronium formation channel is open in the Ore gap (the region between the positronium threshold and the first excitation threshold of the target).

With the advent of more intense positron beams, there has been renewed interest in these processes with new measurements and calculations of many different cross sections being carried out with the noble gases being of particular interest. Primarily for this reason, we have only shown here, the most recent measurements and theoretical calculations. Similarly, more sophisticated theoretical methods have been developed for the determination of both elastic and inelastic cross sections, including positronium formation, for the noble gases [13], [7] and [5] as well as for group II atoms ([3] and [12]). In this paper, we have applied the relativistic optical potential (ROP) method ([4]), hereafter referred to as I, to the scattering of positrons from krypton and xenon from threshold to 1 keV. We have calculated elastic, momentum transfer, viscosity, positronium formation, excitation, direct and total ionization cross sections as well as the grand total cross section. We have used the technique given in McEachran and Stauffer [6] to account for positronium formation in both its ground as well as excited states. We compare these krypton and xenon cross sections to the recommended cross sections presented in Ratnavelu et al. [11] which were determined using all existing experimental and theoretical results.

2 Theory

The theoretical procedures used in this paper to describe the elastic and inelastic scattering of positrons from krypton and xenon atoms were based upon the relativistic optical potential (ROP) method of Chen et al. [4]. Since this ROP method has previously been described in the literature only a brief discussion of the overall method will be given here and the reader is referred to ref. I as well as McEachran and Stauffer [6], hereafter referred to as II, for the details.

In the ROP method, the scattering of the incident positrons by closed-shell atoms is described by the integral equation formulation of the partial wave Dirac–Fock scattering equations (see Eq. (1) of II). Here, the local scattering potential is given by the sum of the static and a local polarization potential. Once again, we have followed the procedure outlined by Bartschat et al. [1,2] and have replaced the real part of the optical potential by a local polarization potential based upon the polarized-orbital method of McEachran et al. [8,9]. The static potentials were determined in the usual manner from the ground state Dirac–Fock orbitals of krypton and xenon while the polarization potential $U_{\mathrm{pol}}(r)$ comprised the sum of the first six multipoles for krypton and the first eight multipoles for xenon. The inclusion of two additional multipoles for xenon is due to its larger atomic polarizabilities. The imaginary and non-local optical potential describes the absorption of the incident flux into the inelastic channels and thereby

[a] e-mail: Joshua.Machacek@anu.edu.au
(corresponding author)
[b] e-mail: Robert.McEachran@anu.edu.au

describes both excitation and ionization processes. This potential is given by a sum and integration over the bound and continuum states of the atom (see §2.1 below as well as Eq. (21b) of ref. I for details).

The complex scattering phase shifts are determined from the asymptotic form of the large component of the scattering wavefunction. These phase shifts are then used to determine the various elastic and inelastic cross sections (see Eqs. (5)–(9) of II).

2.1 The optical potential

For krypton the following 15 bound excited states, in intermediate coupling notation, 5s[3/2]$_1$, 5s[1/2]$_1$, 5p[1/2]$_0$, 5$\bar{\text{p}}$[1/2]$_0$, 5p[5/2]$_2$, 5p[3/2]$_2$, 5$\bar{\text{p}}$[3/2]$_2$, 4$\bar{\text{d}}$[1/2]$_1$, 4d[3/2]$_1$, 4$\bar{\text{d}}$[3/2]$_1$, 4d[7/2]$_3$, 4$\bar{\text{d}}$[5/2]$_3$, 4d[5/2]$_3$, 6s[3/2]$_1$ and 6s[1/2]$_1$ were included in $U_{\text{opt}}(r)$, in order to simulate excitation processes. Similarly, for xenon, the following 15 bound excited states, 6s[3/2]$_1$, 6s[1/2]$_1$, 6p[1/2]$_0$, 6$\bar{\text{p}}$[1/2]$_0$, 6p[5/2]$_2$, 6p[3/2]$_2$, 6$\bar{\text{p}}$[3/2]$_2$, 5$\bar{\text{d}}$[1/2]$_1$, 5d[3/2]$_1$, 5$\bar{\text{d}}$[3/2]$_1$, 5d[7/2]$_3$, 5$\bar{\text{d}}$[5/2]$_3$, 5d[5/2]$_3$, 7s[3/2]$_1$ and 7s[1/2]$_1$ were included in $U_{\text{opt}}(r)$, in order to simulate excitation processes.

Also included in $U_{\text{opt}}(r)$ were all continuum states with orbital angular momentum given by $l_c = 0, 1, 2, 3$ and 4 in order to simulate ionization processes (including Ps formation). The integration over the continuum states in the absorption potential was approximated by using Gauss–Legendre integration usually with 16 points. In a relativistic close coupling expansion, it is necessary to couple the total angular momentum of the electron in the excited state (bound or continuum) to the total angular momentum of the incident positron in order to obtain the total angular momentum J of the positron-atom system. This total angular momentum J is then conserved during the collision process. Under the above circumstances this gave rise to a maximum of 59 excitation channels and 34 ionization channels in $U_{\text{opt}}(r)$ for both krypton and xenon.

2.2 Positronium formation

Positronium formation was simulated using the method given in McEachran and Stauffer [6]. Here, the Ps formation cross section in the ground state is determined by first calculating the direct ionization cross section and then the comparable cross section when the ionization threshold is reduced by 6.8 eV, the binding energy of positronium. The Ps formation cross section is then taken to be the difference between these two results. Similarly, Ps formation in an excited state with principle quantum number n is simulated by reducing the ionization thresholds by $6.8/n^2$ eV. For further details of this method, the reader is referred to reference II.

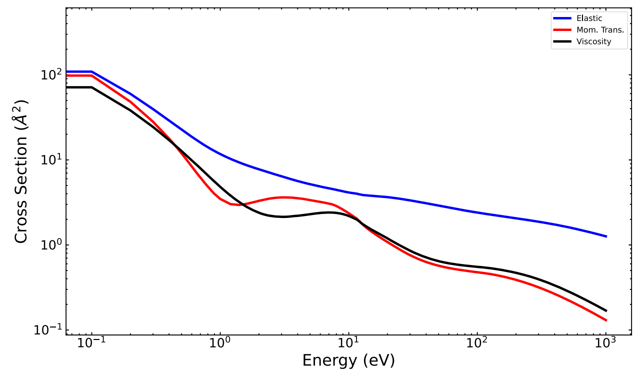

Fig. 1 Elastic scattering (blue curve), momentum transfer (red curve), and viscosity (black curve) cross section for positron scattering from krypton

3 Krypton results

In this section, we show our krypton results and compare with other current calculations and measurements.

3.1 Elastic scattering

For krypton, the energy range where only elastic scattering can occur is from zero to 7.20 eV (the first ionization threshold minus the binding energy of positronium). Since the positron is distinguishable from the constituents of the target, all the phase shifts must be zero at zero energy although the scattering length is nonzero giving rise to a finite nonzero cross section at zero energy. In Fig. 1, we show our present results along with the momentum transfer and viscosity cross sections. The latter two cross sections are useful in the determination of transport properties in gases.

3.2 Positronium formation

In the Ore gap (7.20−10.03 eV), positronium formation is the only inelastic channel open but at higher energies excitation and eventually direct ionization of krypton can occur. We present two sets of cross sections for Ps formation, one where the threshold for ionization is lowered to coincide with the threshold for Ps formation in the ground state (Fig. 2) and the second which is the sum of cross sections calculated when the threshold for ionization is successively lowered to coincide with Ps formation into the first three exited states (Fig. 3). Our calculations are compared with the recommended total positronium formation cross section from Ratnavelu et al. [11] in Fig. 2 The calculation does not rise from threshold as quickly as the recommended curve, which is typical of this method. The peak magnitude and position do not agree. However, the high-energy dependence is very similar. The discrepancy is larger than the typical experimental uncertainty by approximately a factor of two. Our calculations for the excited-state positronium formation for the first three excited states are shown in Fig. 3.

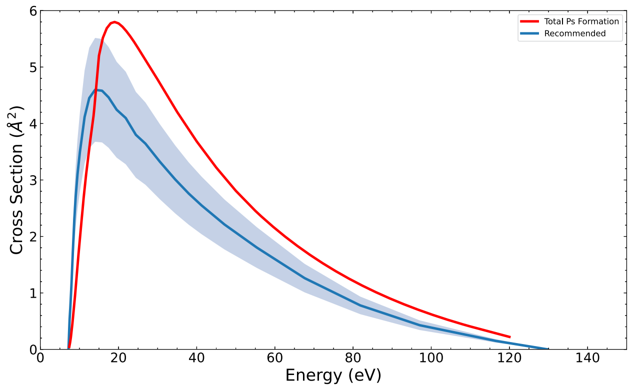

Fig. 2 Total positronium formation cross section for positron scattering from krypton: red curve, present work; blue curve, recommended cross section from review [11]

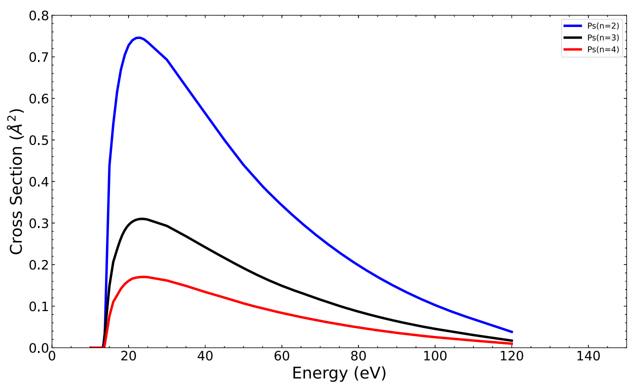

Fig. 3 Excited-state positronium formation cross section for positron scattering from krypton: blue curve, present work for Ps ($n = 2$); black curve, present work for Ps ($n = 3$); red curve, present work for Ps ($n = 4$)

3.3 Electronic excitation

Here, the excitation cross section refers to the sum of the individual excitation cross sections of the 15 excited states, listed above, from the ground state. Thus, either a 4p or $4\bar{p}$ electron from the outermost subshells of the krypton ground state is excited to one of these excited states. Figure 4 shows our results for the total electronic excitation cross sections over the energy range from threshold to 100 eV.

3.4 Direct ionization

The direct ionization cross section refers to the process where both the incident positron and ejected electron are free. Figure 5 shows our results for the direct ionization cross sections over the energy range from threshold to 1 keV. The 4s state is also included above 27.5 eV. Our direct ionization cross section is compared to the recommended cross section of Ratnavelu et al. [11]. These results are consistent to the level of the quoted uncertainty.

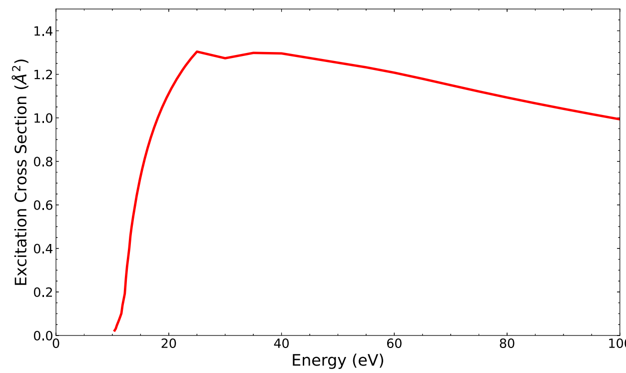

Fig. 4 Excitation cross section for positron scattering from krypton: red curve, present work for the total excitation cross section

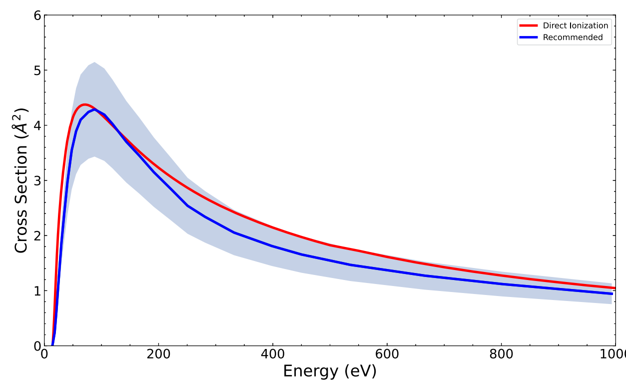

Fig. 5 Direct ionization cross section for positron scattering from krypton: red curve, present work; blue curve, recommended cross section from review [11]

3.5 Grand total cross section

This term refers to the total scattering cross section and is the sum of cross sections for all allowed processes, elastic and inelastic. Figure 6 compares our results with the measurements of Ratnavelu et al. [11]. There is general agreement between the recommended values and the present results except in the near threshold region for positronium formation.

4 Xenon results

In this section, we show our xenon results and compare with more current calculations and measurements.

4.1 Elastic scattering

For xenon, the elastic energy regime is from zero to 5.33 eV. In Fig. 7, we show our present results for the elastic scattering, momentum transfer, and viscosity cross sections.

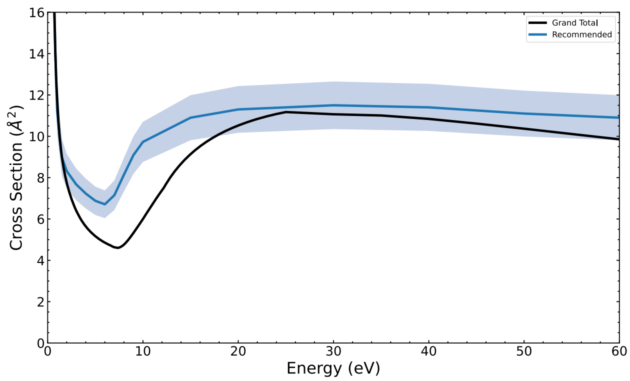

Fig. 6 Grand total cross section for positron scattering from krypton: solid black curve, present work; blue curve, recommended grand total cross section [11]

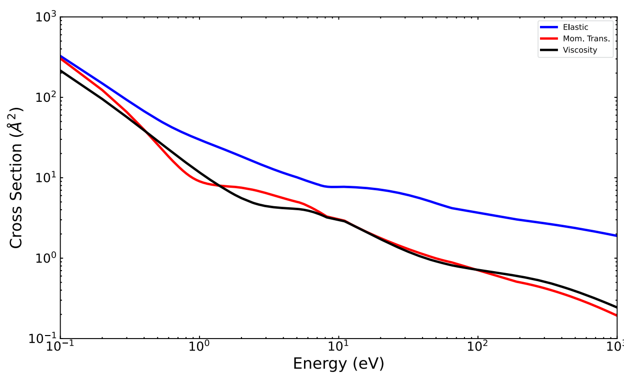

Fig. 7 Elastic scattering (blue curve), momentum transfer (red curve), and viscosity (black curve) cross section for positron scattering from xenon

4.2 Positronium formation

Here, the Ore gap for positronium formation is from 5.33 to 8.44 eV. Once again, we present two sets of cross sections for Ps formation, one corresponding to Ps formation in the ground state ($n = 1$) only and the other corresponding to Ps formation in the first four states ($n = 1 - 4$). Our calculations are compared with the recommended total positronium formation cross section from Ratnavelu et al. [11] in Fig. 8 The calculation does not rise from threshold as quickly as the recommended curve, which is typical of this method. In this case, the peak magnitude agrees but the position is about 5 eV higher. However, the high-energy dependence is very similar with a discrepancy which is larger than the typical experimental uncertainty. Our calculations for the excited-state positronium formation for the first three excited states are shown in Fig. 9. The Ps($n = 2$) experimental and theoretical results are presented in Murtagh et al. [10]. Our results are nearly a factor of two larger than the previously reported theoretical results. However, the relatively large uncertainties from the pioneering experimental results limit a detailed discussion.

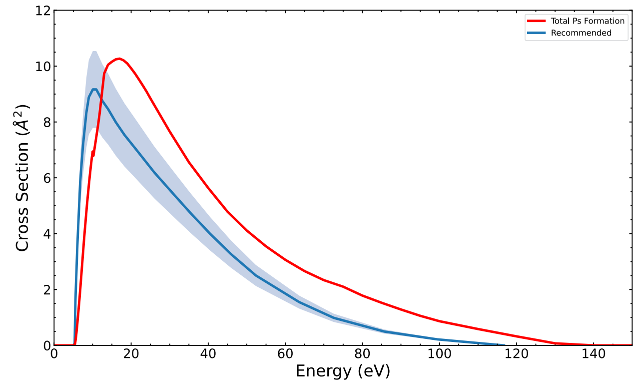

Fig. 8 Total positronium formation cross section for positron scattering from xenon: red curve, present work; blue curve, recommended cross section from review 4 [11]

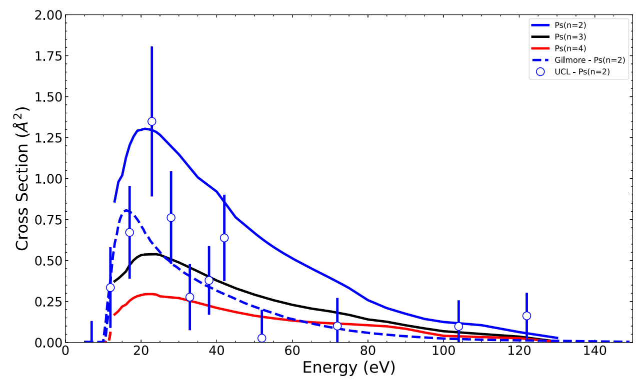

Fig. 9 Excited-state positronium formation cross section for positron scattering from xenon: blue curve, present work for Ps ($n = 2$); blue circles, experimental results from Murtagh et al.; blue dashed curve, theoretical results presented in Murtagh et al.; black curve, present work for Ps($n = 3$); red curve, present work for Ps ($n = 4$)

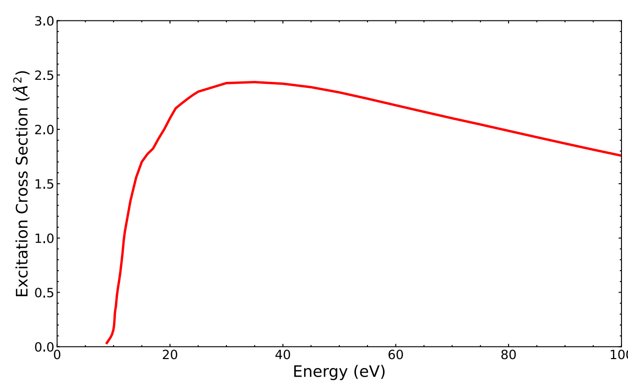

Fig. 10 Excitation cross section for positron scattering from xenon: red curve, present work for the total excitation cross section

4.3 Electronic excitation

Here, the excitation cross section refers to the sum of the individual excitation cross sections of the 15 excited

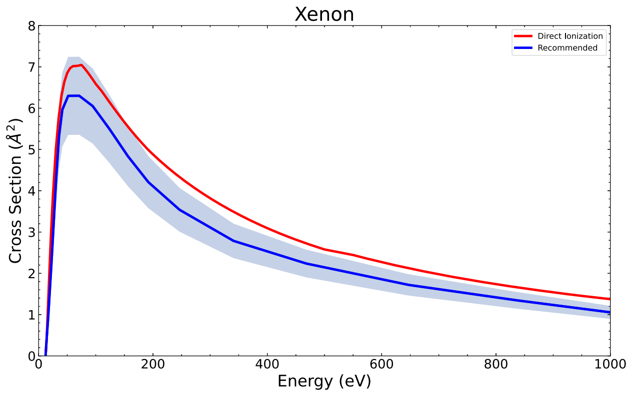

Fig. 11 Direct ionization cross section for positron scattering from xenon: red curve, present work; blue curve, recommended cross section from review [11]

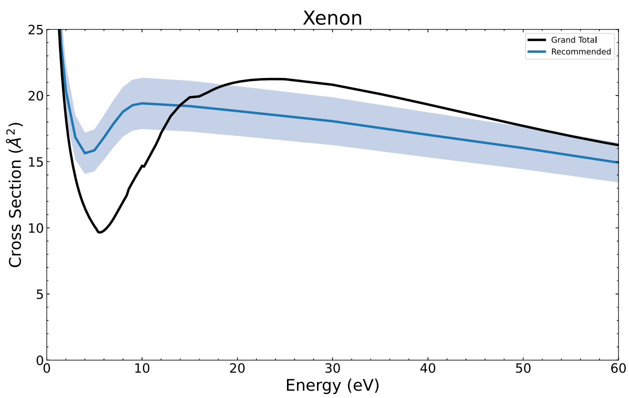

Fig. 12 Grand total cross section for positron scattering from xenon: black curve, present work; red curve, present work for the elastic scattering cross section; blue curve, recommended cross section from review [11]

states of xenon, listed above, from the ground state. Thus, either a 5p or 5$\bar{\text{p}}$ electron from the outermost subshells of the xenon ground state is excited to one of these excited states. Figure 10 shows our results for these electronic excitation cross sections over the energy range from threshold to 100 eV.

4.4 Direct ionization

The direct ionization cross section refers to the process where both the incident positron and ejected electron are free. Figure 11 shows our results for direct ionization cross sections over the energy range from threshold to 1 keV. Above 23.3 eV the 5 s state is also included in this calculation. Our direct ionization cross section is compared to the recommended cross section of Ratnavelu et al. [11]. These results are consistent to the level of the quoted uncertainty up to about 200 eV. However, as the collision energy increases above 200 eV, a systematic difference is evident.

4.5 Grand total cross section

Once again, this term refers to the total scattering cross section and theoretically is the sum of cross sections for all allowed processes, elastic and inelastic. Figure 12 compares our results with the recommended cross section of Ratnavelu et al. [11]. The low and high energy regions are in reasonable agreement. However, from the positronium formation threshold until the peak in the direct ionization, the cross section has largely different dependence.

5 Conclusions

We have presented positron scattering cross sections for collisions with the heavier noble gases krypton and xenon. Over all there is reasonable agreement between the present calculations and the corresponding recommended cross sections found in the literature. The discrepancies present are typically found at, or near, the opening of a new scattering or production channel. In the case of excited-state positronium formation, the large experimental uncertainties limit a detailed discussion. This work highlights the need for more experimental determinations of state-specific cross sections.

Acknowledgements JRM is grateful for financial support from Australian Research Council.

Author contributions

All authors contributed to the conceptualization, calculations, analysis and the writing of this manuscript.

Funding Information Open Access funding enabled and organized by CAUL and its Member Institutions.

Data availability Statement Data will be made available upon reasonable request. The manuscript has associated data in a data repository.

References

1. K. Bartschat, R.P. McEachran, A.D. Stauffer, J. Phys. B At. Mol. Phys. **21**, 2789–2800 (1988)
2. K. Bartschat, R.P. McEachran, A.D. Stauffer, J. Phys. B At. Mol. Phys. **23**, 2349–2355 (1990)
3. F. Blanco, G. Garcia, R.P. McEachran, P.W. Stokes, R.D. White, M.J. Brunger, J. Phys. Chem. Ref. Data **48**, 033103 (2019)
4. S. Chen, R.P. McEachran, A.D. Stauffer, J. Phys. B At. Mol. Phys. **41**, 025201 (2008)
5. J.R. Machacek, R.P. McEachran, Eu. J. Phys. D Brunger Memorial (2023) **(manuscript is in review)**
6. R.P. McEachran, A.D. Stauffer, J. Phys. B At. Mol. Phys. **46**, 075203 (2013)
7. R.P. McEachran, A.D. Stauffer, J. Phys. B At. Mol. Phys. **52**, 115203 (2019)
8. R.P. McEachran, D.L. Morgan, A.G. Ryman, A.D. Stauffer, J. Phys. B At. Mol. Opt. Phys. **10**, 663 (1977)
9. R.P. McEachran, D.L. Morgan, A.G. Ryman, A.D. Stauffer, J. Phys. B At. Mol. Opt. Phys. **11**, 951 (1978)
10. D.J. Murtagh, D.A. Cooke, G. Laricchia, Phys. Rev. Lett. **102**, 133–202 (2009)
11. K. Ratnavelu, M.J. Brunger, S.J. Buckman, J. Phys. Chem. Ref. Data **48**, 023102 (2019)
12. P.W. Stokes, R.D. White, R.P. McEachran, F. Blanco, G. Garcia, M.J. Brunger, J. Phys. Chem. Ref. Data **50**, 023101 (2021)
13. R. Utamuratov, A.S. Kadyrov, D.V. Fursa, I. Bray, J. Phys. B At. Mol. Phys. **43**, 031001 (2010)